Conservative arbitrary order finite difference schemes for shallow-water flows

Yuri N. Skiba[a], Denis M. Filatov[b],*

[a]*Center for Atmospheric Science (CCA), National Autonomous University of Mexico (UNAM), Circuito Exterior, C.P. 04510 Mexico City, Mexico*
[b]*Center for Computing Research (CIC), National Polytechnic Institute (IPN), C.P. 07738 Mexico City, Mexico*

Abstract

The classical nonlinear shallow-water model (SWM) of an ideal fluid is considered. For the model, a new method for the construction of mass and total energy conserving finite difference schemes is suggested. In fact, it produces an infinite family of finite difference schemes, which are either linear or nonlinear depending on the choice of certain parameters. The developed schemes can be applied in a variety of domains on the plane and on the sphere. The method essentially involves splitting of the model operator by geometric coordinates and by physical processes, which provides substantial benefits in the computational cost of solution. Besides, in case of the whole sphere it allows applying the same algorithms as in a doubly periodic domain on the plane and constructing finite difference schemes of arbitrary approximation order in space. Results of numerical experiments illustrate the skillfulness of the schemes in describing the shallow-water dynamics.
© 2007 Elsevier B.V. All rights reserved.

Keywords: Conservative finite difference schemes; Operator splitting; Shallow-water equations

1. Introduction

Consider the classical shallow-water system in the spherical coordinates (λ, φ) written in the divergent form [17]

$$\frac{\partial U}{\partial t} + \frac{1}{R\cos\varphi}\frac{1}{2}\left[\left(\frac{\partial uU}{\partial\lambda} + u\frac{\partial U}{\partial\lambda}\right) + \left(\frac{\partial vU\cos\varphi}{\partial\varphi} + v\cos\varphi\frac{\partial U}{\partial\varphi}\right)\right] - \left(f + \frac{u}{R}\tan\varphi\right)V = -\frac{gz}{R\cos\varphi}\frac{\partial h}{\partial\lambda}, \quad (1)$$

$$\frac{\partial V}{\partial t} + \frac{1}{R\cos\varphi}\frac{1}{2}\left[\left(\frac{\partial uV}{\partial\lambda} + u\frac{\partial V}{\partial\lambda}\right) + \left(\frac{\partial vV\cos\varphi}{\partial\varphi} + v\cos\varphi\frac{\partial V}{\partial\varphi}\right)\right] + \left(f + \frac{u}{R}\tan\varphi\right)U = -\frac{gz}{R}\frac{\partial h}{\partial\varphi}, \quad (2)$$

$$\frac{\partial H}{\partial t} + \frac{1}{R\cos\varphi}\left[\frac{\partial zU}{\partial\lambda} + \frac{\partial zV\cos\varphi}{\partial\varphi}\right] = 0. \quad (3)$$

Here the vector $(u, v)^{\mathrm{T}}$, $u = u(\lambda, \varphi, t)$, $v = v(\lambda, \varphi, t)$, determines the velocity of a fluid, $H = H(\lambda, \varphi, t)$ is the fluid's depth, $f = f(\varphi)$ is the Coriolis acceleration, R is the sphere's radius, $h = h(\lambda, \varphi, t)$ is the free surface height, $z := \sqrt{H}$,

---

* Corresponding author. Tel.: +52 55 5729 6000; fax: +52 55 5586 2936.

E-mail addresses: skiba@servidor.unam.mx (Y.N. Skiba), denisfilatov@gmail.com (D.M. Filatov).

$U := zu$, and $V := zv$. Besides, it holds $h = H + h_r$, where $h_r = h_r(\lambda, \varphi)$ is the underlying relief's height. Problem (1)–(3) is being studied on a sphere S, with λ as the longitude (positive eastward) and φ as the latitude (positive northward).

It is known that the shallow-water equations (SWEs) describing the dynamics of a non-dissipative and unforced fluid conserve such integral characteristics as the mass, total (kinetic plus potential) energy, and potential enstrophy [9,22]. However, numerical solution to SWEs requires a discretization of the continuous equations and a reduction of problem (1)–(3) to a system of finite difference schemes. It is crucial that the discrete analogues of all the invariants of motion usually stop being invariant, and so the numerical solution may contain additional approximation errors and stimulate nonlinear instability [22]. If the norm related to the total energy is not conserved in time then the numerical solution may differ considerably from the exact one, especially in case of long-term integration [6]. In order to avoid the numerical instability effect, conservative finite difference schemes have to be employed [23].

In the last 40 years there have been suggested several finite difference schemes that conserve some or other integral characteristics of the SWEs. Nevertheless, many of these methods treat the temporal derivatives in (1)–(3) as continuous functions, and therefore those schemes stop being conservative when these derivatives are discretized in time and an explicit temporal approximation is used [1,3,4,10,12–14,21]. More precisely, for the fully discrete model (i.e., discrete both in time and in space) the cited methods involve an explicit approximation in time, and hence only first-order integral characteristics, such as the mass, can be conserved. Yet, even if one employs the Crank–Nicolson approximation [2,11] to conserve the energy, the cited methods turn out to be hard-to-implement.

In this paper we develop a new method for the numerical simulation of shallow-water flows. The method permits conserving the mass and the total energy for the fully discrete shallow-water systems, as well as can be used both in the Cartesian and spherical geometries [17,19,20]. The method essentially involves splitting of the model operator by geometric coordinates and by physical processes [7,8], which provides substantial benefits in the computational cost of solution. Yet, in case of the whole sphere it allows applying the same algorithms as in a doubly periodic domain on the plane. The latter is achieved due to the joint use of the splitting method and two different coordinate maps that leads to solving one-dimensional problems with periodic conditions in each direction. As a result, the numerical algorithm for the whole sphere does not differ from the corresponding algorithm for a doubly periodic domain on the plane. In particular, finite difference schemes of arbitrary approximation order in space can easily be constructed for the whole sphere in the same way as for a doubly periodic planar domain. Due to specially chosen spatial approximations, each split system conserves the mass and the total energy. In fact, an infinite family of such schemes is suggested, which are either linear or nonlinear depending on the choice of certain parameters.

Because of the rigid restrictions on the size of a journal article we will consider the SWEs only on a sphere. A detailed study of the Cartesian case can be found in [19]. We plan to consider hydrodynamic (initial boundary value) problems in the next work. However, one particular case of such limited area problems, namely SWEs in a periodic channel on a sphere, will be considered in the present paper as well.

2. Crank–Nicolson approximation and operator splitting

The differential operator of the shallow-water model (SWM) as a closed system without sources and sinks of energy is an antisymmetric operator. In order to construct conservative finite difference schemes, we apply coordinate splitting of the model operator and separate the process of sphere rotation. Then, we employ the well-known fact that in case of an evolutional closed system

$$\frac{\partial \overline{\xi}}{\partial t} + A\overline{\xi} = 0 \tag{4}$$

with an antisymmetric operator A [5], the only two-layered scheme of the form

$$\frac{\overline{\xi}^{n+1} - \overline{\xi}^n}{\tau} + A(\alpha\overline{\xi}^{n+1} + (1-\alpha)\overline{\xi}^n) = 0, \quad 0 \leqslant \alpha \leqslant 1, \tag{5}$$

keeping the solution's norm constant is the Crank–Nicolson approximation ($\alpha = \frac{1}{2}$) [2]. Although the Crank–Nicolson scheme is dispersive, this feature is effectively controlled by taking the timestep sufficiently small [11]. So, defining
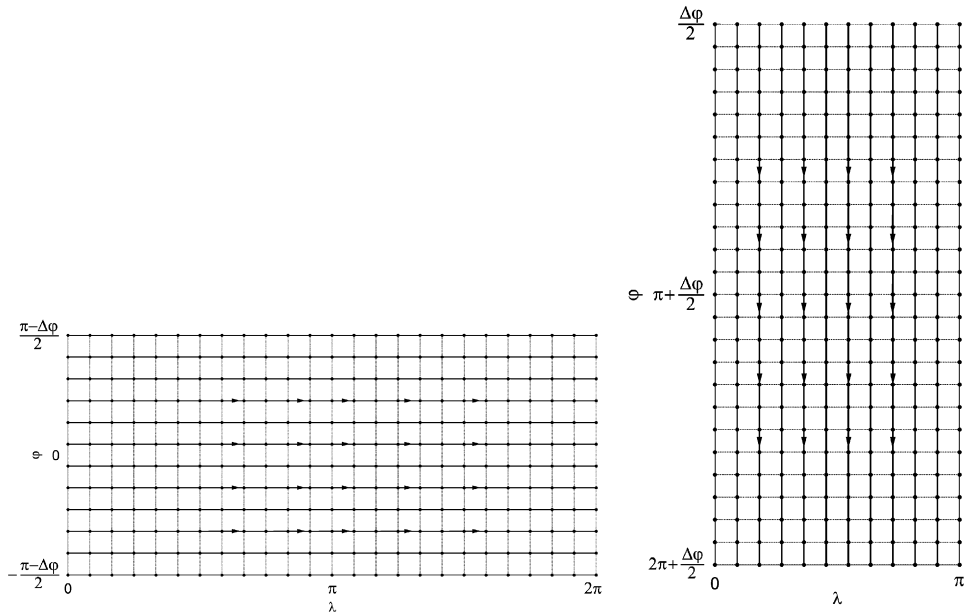
Fig. 1. The coordinate splitting allows representing the sphere in two different forms, merely by swapping the coordinates $(\lambda, \varphi) \rightleftarrows (\varphi, \lambda)$. This permits to use the same algorithm for computing the solution in every direction, keeping the $(2N + 1)$-diagonal structure of the matrices. The black arrows show the direction of calculations.

$\tau = t_{n+1} - t_n$, $\Delta\lambda = \lambda_{k+1} - \lambda_k$, $\Delta\varphi = \varphi_{l+1} - \varphi_l$, $W_{kl}^n = W(\lambda_k, \varphi_l, t_n)$, as well as

$$W_{kl} = \frac{W_{kl}^{n+1} + W_{kl}^n}{2}, \tag{6}$$

where the symbol W is substituted by the functions h, H, U, V, u, v, and z, we cover the sphere S as follows:

$$S_{\Delta\lambda, \Delta\varphi}^{(1)} = \left\{ (\lambda_k, \varphi_l) : \lambda_k \in [0, 2\pi), \varphi_l \in \left[-\frac{\pi}{2} + \frac{\Delta\varphi}{2}, \frac{\pi}{2} - \frac{\Delta\varphi}{2} \right] \right\}, \tag{7}$$

excluding the pole singularities [23], and involve the operator splitting, first considering the equations with respect to the coordinate λ, then in φ, and finally taking into account the Coriolis terms. For example, for the second-order central finite difference scheme in λ we will obtain (the second subindex, l, is omitted for clarity where possible)

$$\frac{U_k^{n+1} - U_k^n}{\tau} + \frac{1}{2c_l} \left(\frac{\bar{u}_{k+1} U_{k+1} - \bar{u}_{k-1} U_{k-1}}{2\Delta\lambda} + \bar{u}_k \frac{U_{k+1} - U_{k-1}}{2\Delta\lambda} \right) = -\frac{g\bar{z}_k}{c_l} \frac{h_{k+1} - h_{k-1}}{2\Delta\lambda}, \tag{8}$$

$$\frac{V_k^{n+1} - V_k^n}{\tau} + \frac{1}{2c_l} \left(\frac{\bar{u}_{k+1} V_{k+1} - \bar{u}_{k-1} V_{k-1}}{2\Delta\lambda} + \bar{u}_k \frac{V_{k+1} - V_{k-1}}{2\Delta\lambda} \right) = 0, \tag{9}$$

$$\frac{H_k^{n+1} - H_k^n}{\tau} + \frac{1}{c_l} \frac{\bar{z}_{k+1} U_{k+1} - \bar{z}_{k-1} U_{k-1}}{2\Delta\lambda} = 0. \tag{10}$$

(Here $c_l := R \cos\varphi_l$.) The functions $U_{k\pm1}$, $V_{k\pm1}$, and $h_{k\pm1}$ are substituted as it is defined in (6), which yields the Crank–Nicolson approximation. It is noteworthy that although the sphere is obviously *not* a doubly periodic domain, this is exactly the method of splitting that allows applying the same numerical algorithm for solving the SWEs in the direction φ. Indeed, cover the sphere as follows:

$$S_{\Delta\lambda, \Delta\varphi}^{(2)} = \left\{ (\lambda_k, \varphi_l) : \lambda_k \in [0, \pi), \varphi_l \in \left[\frac{\Delta\varphi}{2}, 2\pi + \frac{\Delta\varphi}{2} \right) \right\}. \tag{11}$$
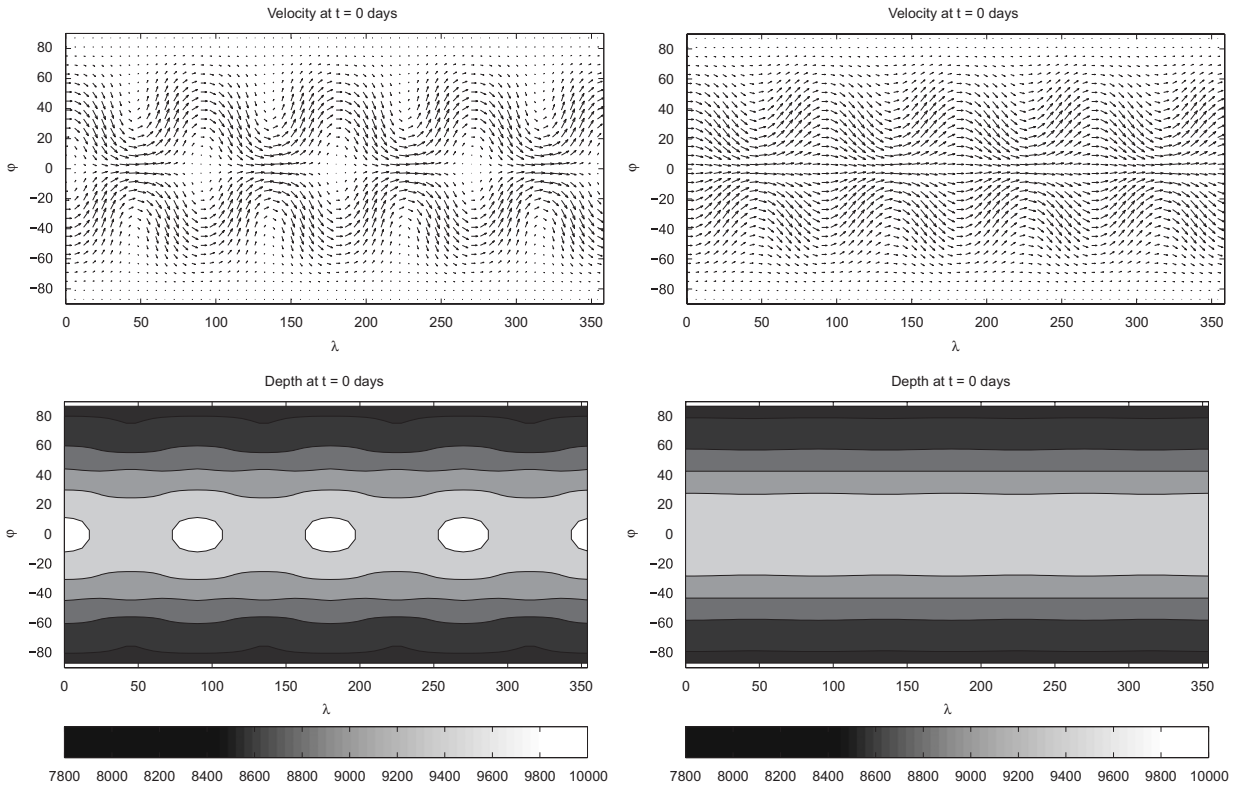
Fig. 2. RH4 initial conditions corresponding to $K = \omega$ (left) and $K = \omega/10$ (right).

It is evident that the grid covering (11) uses the same nodes as in (7). Such a swap of coordinates (because of the splitting) allows using periodic boundary conditions in the φ-direction in the same manner as in the λ-direction (Fig. 1). Therefore we avoid the necessity of imposing adequate boundary conditions at the poles, which is a purely artificial problem caused by the spherical coordinate system. As an alternative one could involve the matrix bordering procedure—first to find the solution at the poles (boundary points) and then at the rest grid points. However, this would not allow constructing high-order (fourth-, sixth-, etc.) finite difference schemes. Unlike these techniques, our approach does allow increasing the approximation order in space up to an arbitrary, even or odd, integer in both directions [18,20]. Besides, the temporal accuracy of the solution can be improved up to the second order [20]. As for the rotation process, we will have

$$\frac{U_{kl}^{n+1} - U_{kl}^{n}}{\tau} - \left(f_l + \frac{\overline{u}_{kl}}{R} \tan \varphi_l \right) V_{kl} = 0, \tag{12}$$

$$\frac{V_{kl}^{n+1} - V_{kl}^{n}}{\tau} + \left(f_l + \frac{\overline{u}_{kl}}{R} \tan \varphi_l \right) U_{kl} = 0. \tag{13}$$

Expressing from (10) H_k^{n+1} and substituting $h_k^{n+1} = H_k^{n+1} + h_{rk}$ into (8), we will get

$$\frac{U_k^{n+1} - U_k^{n}}{\tau} + P_1 + P_2 = P_3 + P_4, \tag{14}$$

where

$$P_1 = \frac{1}{8c_l \Delta \lambda} S_1(n+1), \quad P_2 = -\frac{\tau g \overline{z}_k}{16 c_l^2 \Delta \lambda^2} S_2(n+1),$$

$$P_3 = -\frac{1}{8c_l \Delta \lambda} S_1(n), \quad P_4 = -\frac{g \overline{z}_k}{4 c_l \Delta \lambda} \left(2(h_{k+1}^n - h_{k-1}^n) - \frac{\tau}{4 c_l \Delta \lambda} S_2(n) \right),$$

Table 1
Maximum variation (in %) of the potential enstrophy, $K = \omega$

Grid	Second	Fourth
$12° \times 12°$	2.708	1.699
$6° \times 6°$	0.768	0.642
$3° \times 3°$	0.431	0.365
$1.5° \times 1.5°$	0.290	0.243

Table 2
Maximum variation (in %) of the potential enstrophy, $K = \omega/10$

Grid	Second	Fourth
$12° \times 12°$	2.233	1.302
$6° \times 6°$	0.575	0.461
$3° \times 3°$	0.231	0.195
$1.5° \times 1.5°$	0.094	0.071

and

$$S_1(n) = (\overline{u}_{k+1} + \overline{u}_k)U_{k+1}^n - (\overline{u}_{k-1} + \overline{u}_k)U_{k-1}^n,$$

$$S_2(n) = \overline{z}_{k+2}U_{k+2}^n - 2\overline{z}_k U_k^n + \overline{z}_{k-2}U_{k-2}^n.$$

If we now define

$$\overline{u}_{kl} = u_{kl}, \quad \overline{v}_{kl} = v_{kl}, \quad \overline{z}_{kl} = z_{kl}, \tag{15}$$

where u_{kl}, v_{kl}, and z_{kl} are also substituted via (6), then all the schemes will remain nonlinear; if

$$\overline{u}_{kl} = u_{kl}^n, \quad \overline{v}_{kl} = v_{kl}^n, \quad \overline{z}_{kl} = z_{kl}^n, \tag{16}$$

then all the schemes will reduce to $(2N + 1)$-diagonal systems of linear algebraic [19,20] (here N is the spatial approximation order). For the Coriolis terms we hence also obtain explicit formulas

$$U_{kl}^{n+1} = \frac{\left(1 - \dfrac{\tau^2}{4}\left(f_l + \dfrac{\overline{u}_{kl}}{R}\tan\varphi_l\right)^2\right)U_{kl}^n + \tau\left(f_l + \dfrac{\overline{u}_{kl}}{R}\tan\varphi_l\right)V_{kl}^n}{1 + \dfrac{\tau^2}{4}\left(f_l + \dfrac{\overline{u}_{kl}}{R}\tan\varphi_l\right)^2}, \tag{17}$$

$$V_{kl}^{n+1} = \frac{\left(1 - \dfrac{\tau^2}{4}\left(f_l + \dfrac{\overline{u}_{kl}}{R}\tan\varphi_l\right)^2\right)V_{kl}^n - \tau\left(f_l + \dfrac{\overline{u}_{kl}}{R}\tan\varphi_l\right)U_{kl}^n}{1 + \dfrac{\tau^2}{4}\left(f_l + \dfrac{\overline{u}_{kl}}{R}\tan\varphi_l\right)^2}. \tag{18}$$

Because we employed the Crank–Nicolson approximation, all the derived schemes possess the mass and total energy conservation laws [18–20]. For example, multiplying (10) by $\tau\Delta\lambda$, summing over all the k's, and taking into account
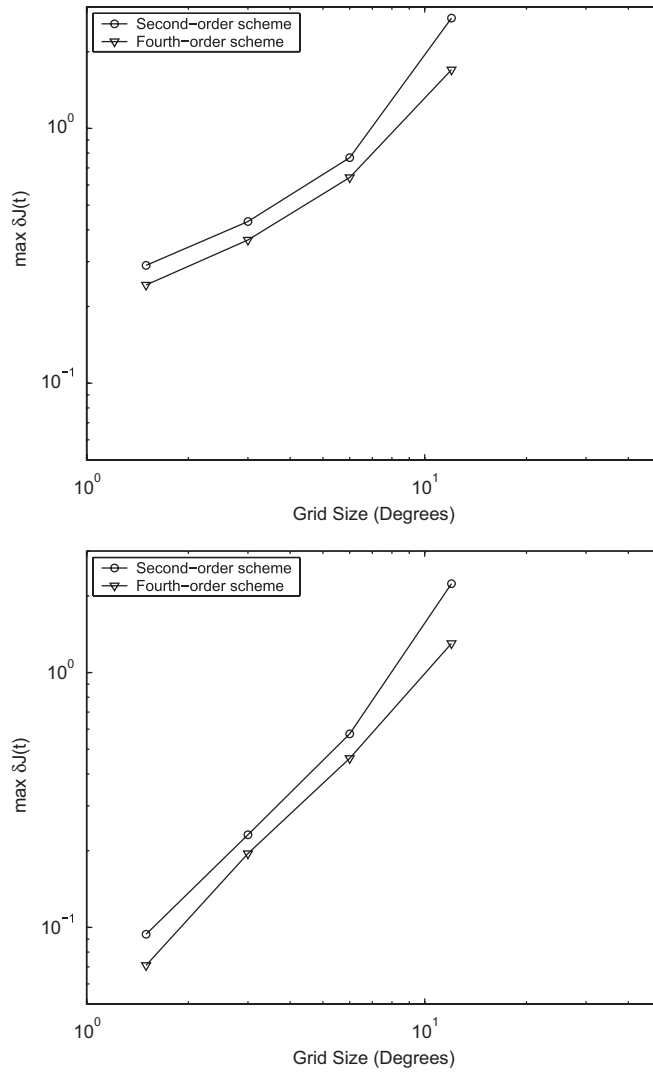
Fig. 3. Convergence rate of the second-order and fourth-order schemes; $K = \omega$ (top) and $K = \omega/10$ (bottom).

the periodic boundary conditions in λ, we have (l is fixed)

$$M_l^{n+1} = \Delta\lambda \sum_k H_{kl}^{n+1} = \cdots = \Delta\lambda \sum_k H_{kl}^n = M_l^n, \tag{19}$$

which shows that the mass conserves in λ. Further, multiplying (8) by $\tau\Delta\lambda U_{kl}$, (9) by $\tau\Delta\lambda V_{kl}$, and (10) by $\tau\Delta\lambda g h_{kl}$, summing in k, and taking into account the periodicity, we obtain

$$E_l^{n+1} = \Delta\lambda \sum_k \frac{1}{2}([U_{kl}^{n+1}]^2 + [V_{kl}^{n+1}]^2 + g([h_{kl}^{n+1}]^2 - [h_{r,kl}]^2))$$

$$= \cdots = \Delta\lambda \sum_k \frac{1}{2}([U_{kl}^n]^2 + [V_{kl}^n]^2 + g([h_{kl}^n]^2 - [h_{r,kl}]^2)) = E_l^n, \tag{20}$$

that is the energy conserves in λ too. Here we substantially use the properties of divergent form of the shallow-water system [15,16]. Analogous results can be obtained in the second direction, while system (12)–(13) (or (17)–(18) as well) does not affect the conservation laws. Thus, the derived schemes conserve both the mass and the total energy.
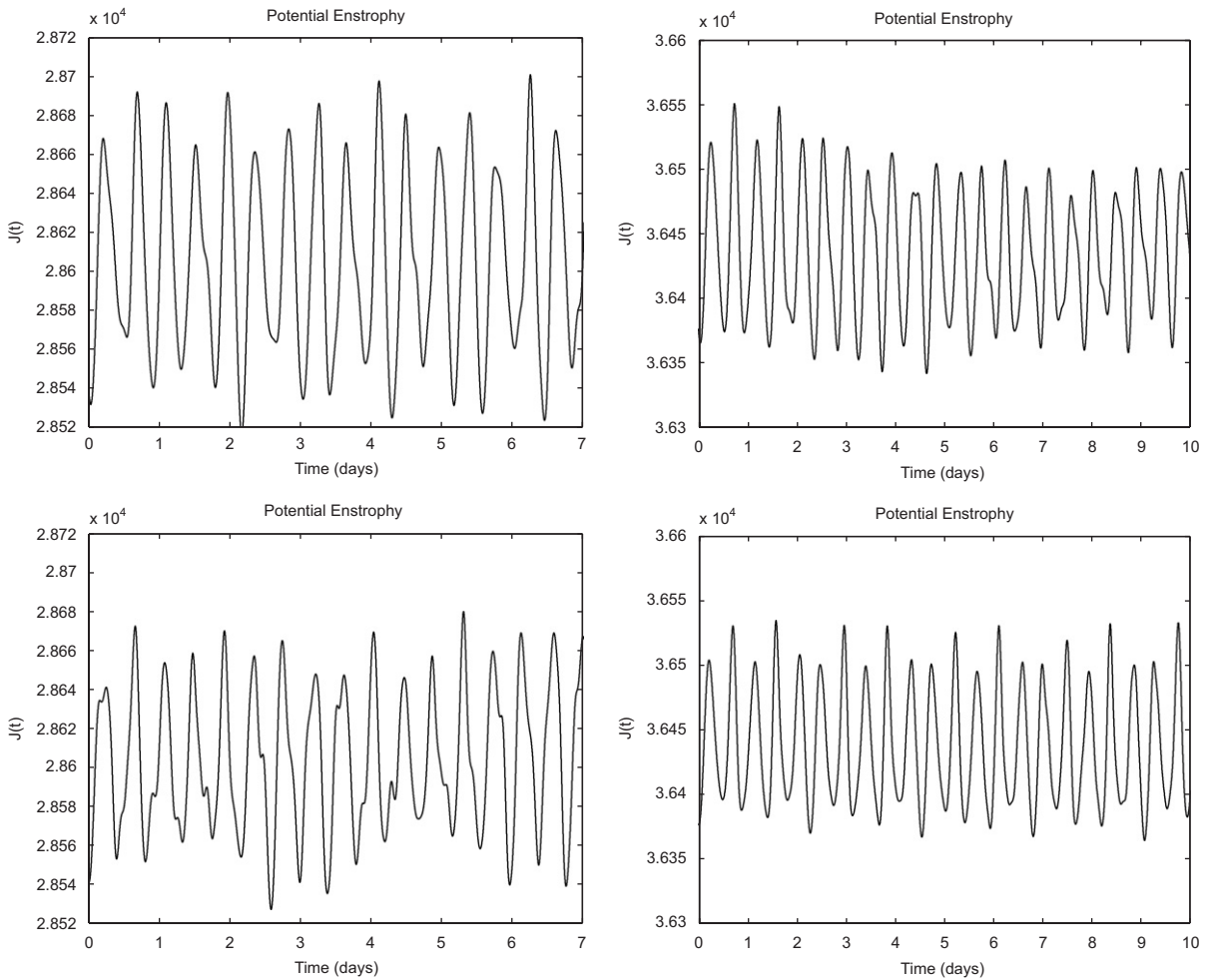
Fig. 4. Behavior of the potential enstrophy in time on the grid $6° \times 6°$. Second-order (top) and fourth-order schemes (bottom); $K = \omega$ (left) and $K = \omega/10$ (right).

It is to stress that since under (16) all the conservative schemes are systems of linear algebraic equations with band $((2N + 1)$-diagonal) matrices, we can apply fast direct band solvers for their inversion [11]. In other words, all the schemes admit a non-iterative solution, keeping the mass and the total energy really constant, while iterative methods would violate the conservation laws.

3. A case of IBVP: periodic channel

The developed approach admits an extension to the case of initial boundary value problem studied in a periodic channel with vanishing second velocity component at the lateral boundary. Namely, consider system (1)–(3) subject to the appropriate initial conditions on U, V, and H, periodic boundary conditions in λ, and the zero Dirichlet boundary condition on V at the lateral boundary of the channel $C = \{(\lambda, \varphi) : \lambda \in [0, 2\pi), \varphi \in (\varphi_1, \varphi_2)\}$, i.e., $V|_{\varphi=\varphi_1} = V|_{\varphi=\varphi_2} = 0$. In [17] it was shown that if this system is approximated as shown in Section 2, then its mass and total energy will be kept constant during all the time of modeling. Therefore, aside from being applicable both in planar and spherical domains, the developed method is flexible from the geometrical standpoint: it can be used for solving shallow-water problems in doubly periodic domains and periodic channels with zero Dirichlet lateral boundary conditions. It is to stress that these types of problems are met very often while modeling real atmospherical phenomena, such as, e.g., Rossby–Haurwitz waves, flood waves, Kelvin waves propagating at low latitudes along the equator, etc. [22].
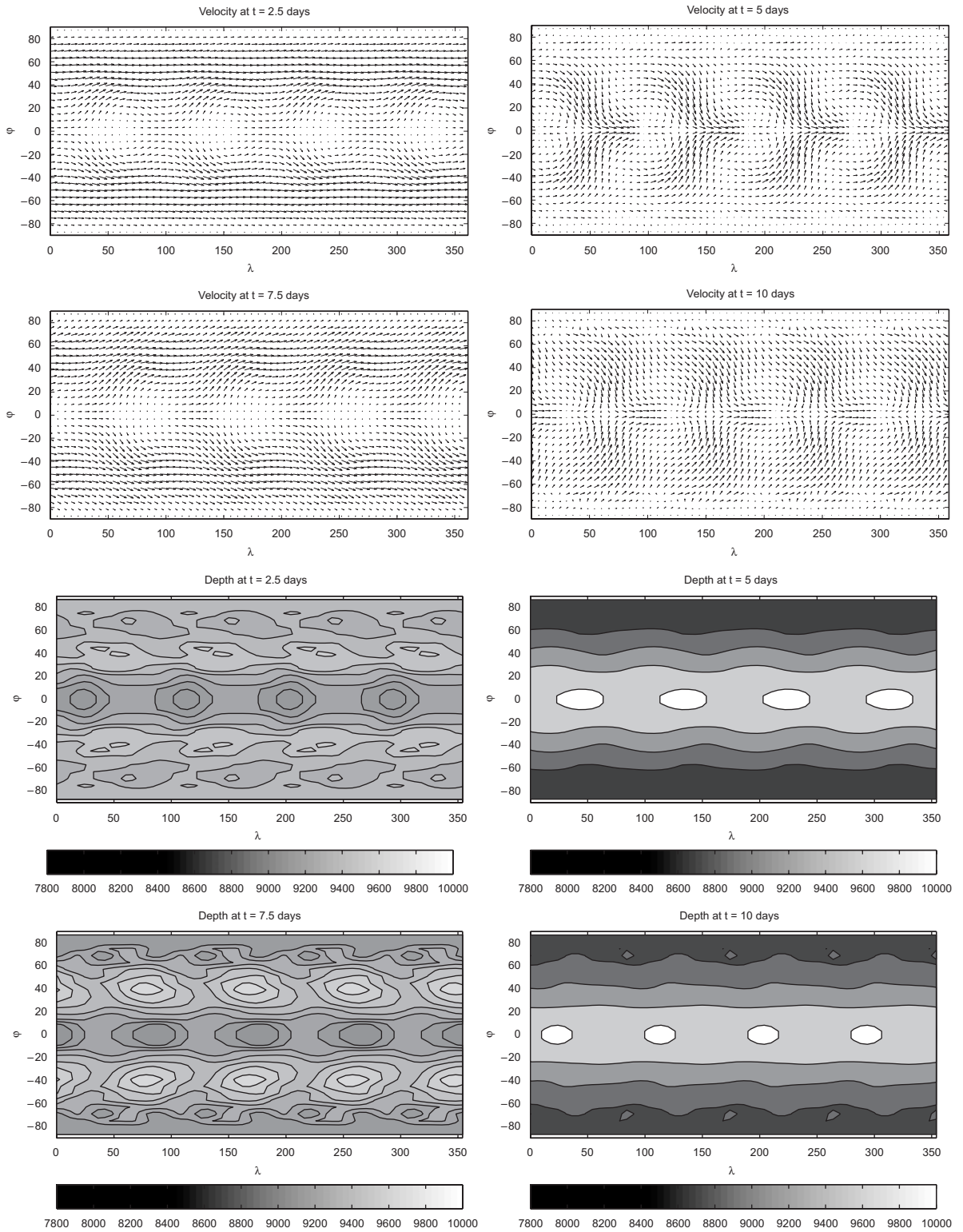
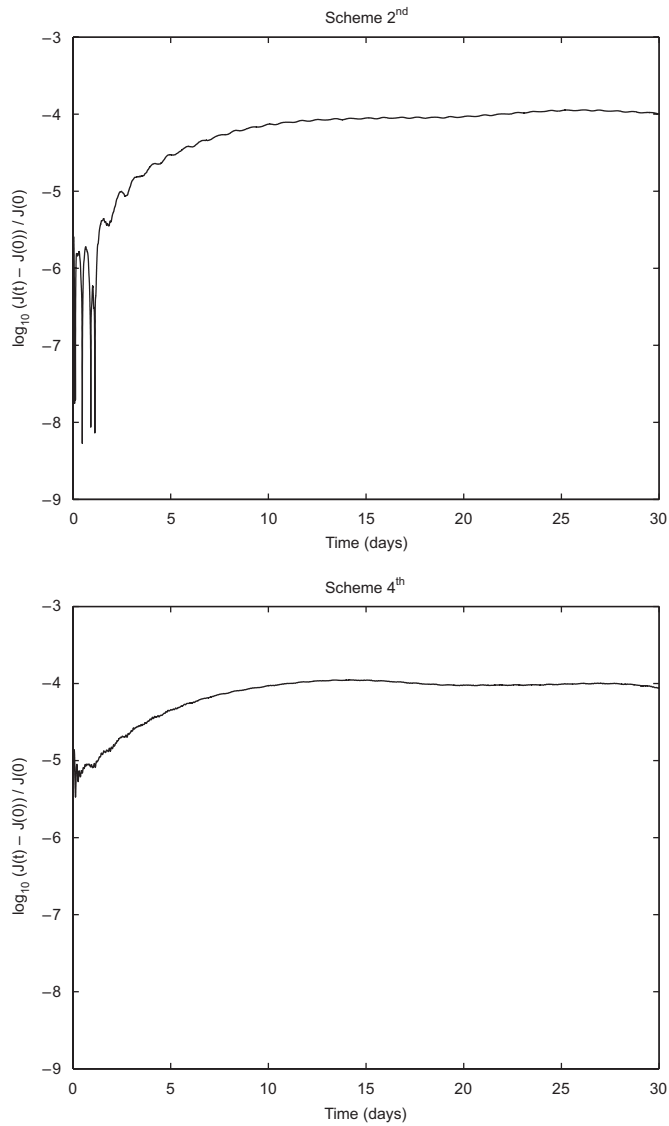Fig. 5. RH4 solutions according to $K = \omega$ at various time moments.

Fig. 6. Plot of $\log_{10}(J(t) - J(0))/J(0)$ for the second-order (top) and fourth-order scheme (bottom).

It should be recognized, however, that the most general case of initial boundary value problems is more complicated, and further studies are needed here. Such kind of problems are principally met in hydrodynamics rather than in (global) atmospherical applications. We will leave the question of conservative shallow-water schemes for IBVPs for a future research.

4. Numerical tests

We tested the suggested method with the Rossby–Haurwitz waves having verified the funcionality of the second-order and fourth-order schemes. As the initial condition we took [24]

$$u = R\omega \cos\varphi + RK\cos^{\alpha-1}\varphi(\alpha\sin^2\varphi - \cos^2\varphi)\cos\alpha\lambda, \tag{21}$$

$$v = -RK\alpha\cos^{\alpha-1}\varphi\sin\varphi\sin\alpha\lambda, \tag{22}$$

$$gh = gh_0 + R^2 A(\varphi) + R^2 B(\varphi)\cos\alpha\lambda + R^2 C(\varphi)\cos 2\alpha\lambda, \tag{23}$$
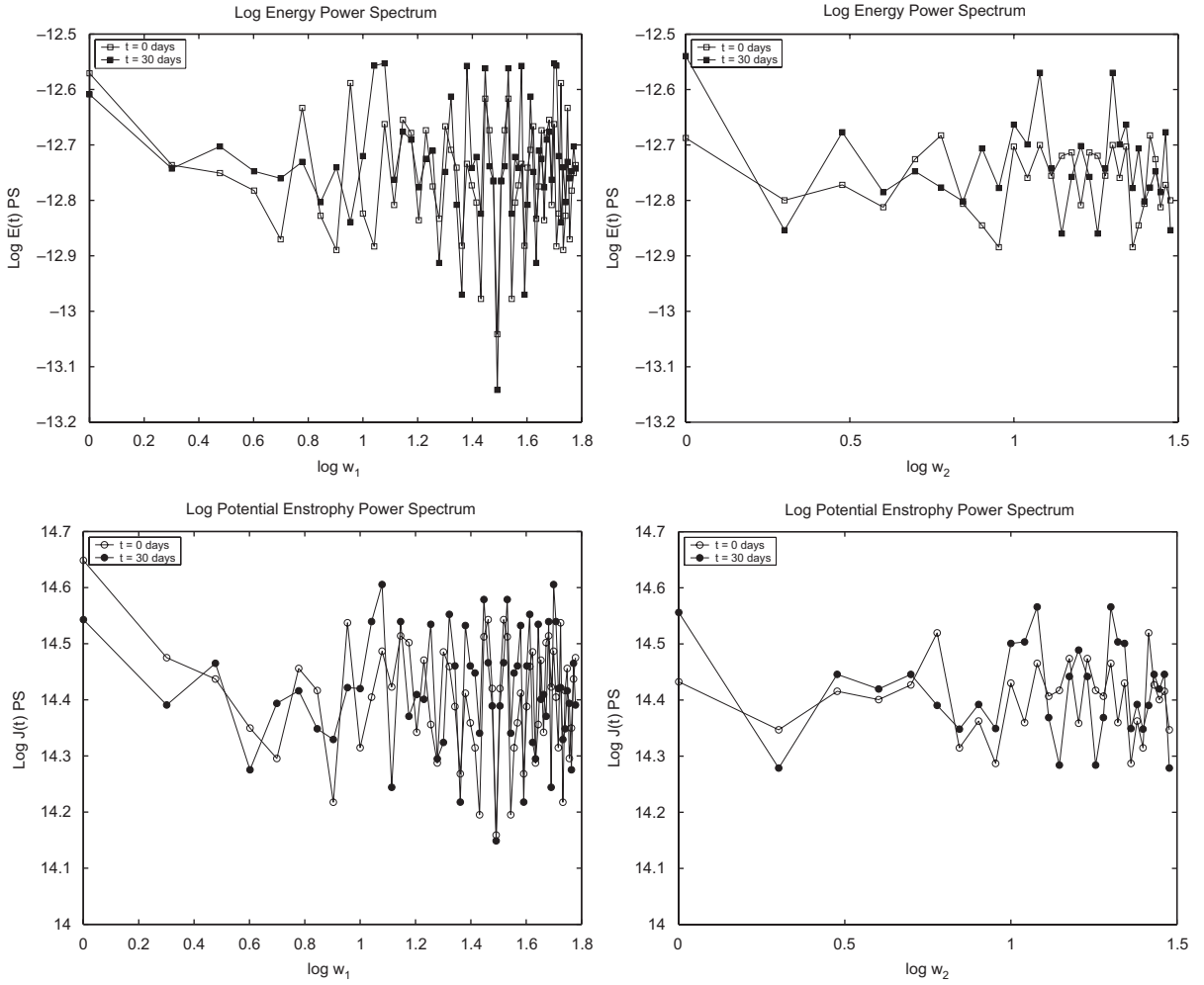
Fig. 7. Power spectra of the total energy (top) and potential enstrophy (bottom) at $t = 0$ and 30 days, second-order scheme. The results are averaged in ω_2 (left) and ω_1 (right).

where

$$A(\varphi) = \frac{\omega}{2}(2\Omega + \omega)\cos^2\varphi + \frac{1}{4}K^2\cos^{2\alpha}\varphi((\alpha + 1)\cos^2\varphi + (2\alpha^2 - \alpha - 2) - 2\alpha^2\cos^{-2}\varphi), \tag{24}$$

$$B(\varphi) = \frac{2(\Omega + \omega)K}{(\alpha + 1)(\alpha + 2)}\cos^\alpha\varphi((\alpha^2 + 2\alpha + 2) - (\alpha + 1)^2\cos^2\varphi), \tag{25}$$

$$C(\varphi) = \frac{1}{4}\alpha^2\cos^{2\alpha}\varphi((\alpha + 1)\cos^2\varphi - (\alpha + 2)). \tag{26}$$

We had $h_0 = 8000$ m, the maximum velocity was 10 m/s. We considered the case $\alpha = 4$, $\omega = 7.848 \times 10^{-6}\,\text{s}^{-1}$. We took $K = \omega$ and $K = \omega/10$ (Fig. 2). The parameter K stands for the non-zonal component of the solution; the smaller K the more zonal character of the flow, and vice versa. For different spatial grids the timestep was chosen to be such that the dimensionless grid number was always of order $O(1)$ in order for the finite difference approximations to be accurate.

In Tables 1 and 2 there are maximum variations of the potential enstrophy (define $\|\delta J(t)\|_{C[0,T]} := \max_{t \in (0,T]} \delta J(t)$) for different schemes (in %). It is seen that in both cases the fourth-order scheme provides more accurate solutions than the second-order one. In Fig. 3 we show the convergence rate as a function of the maximum enstrophy variation vs. the
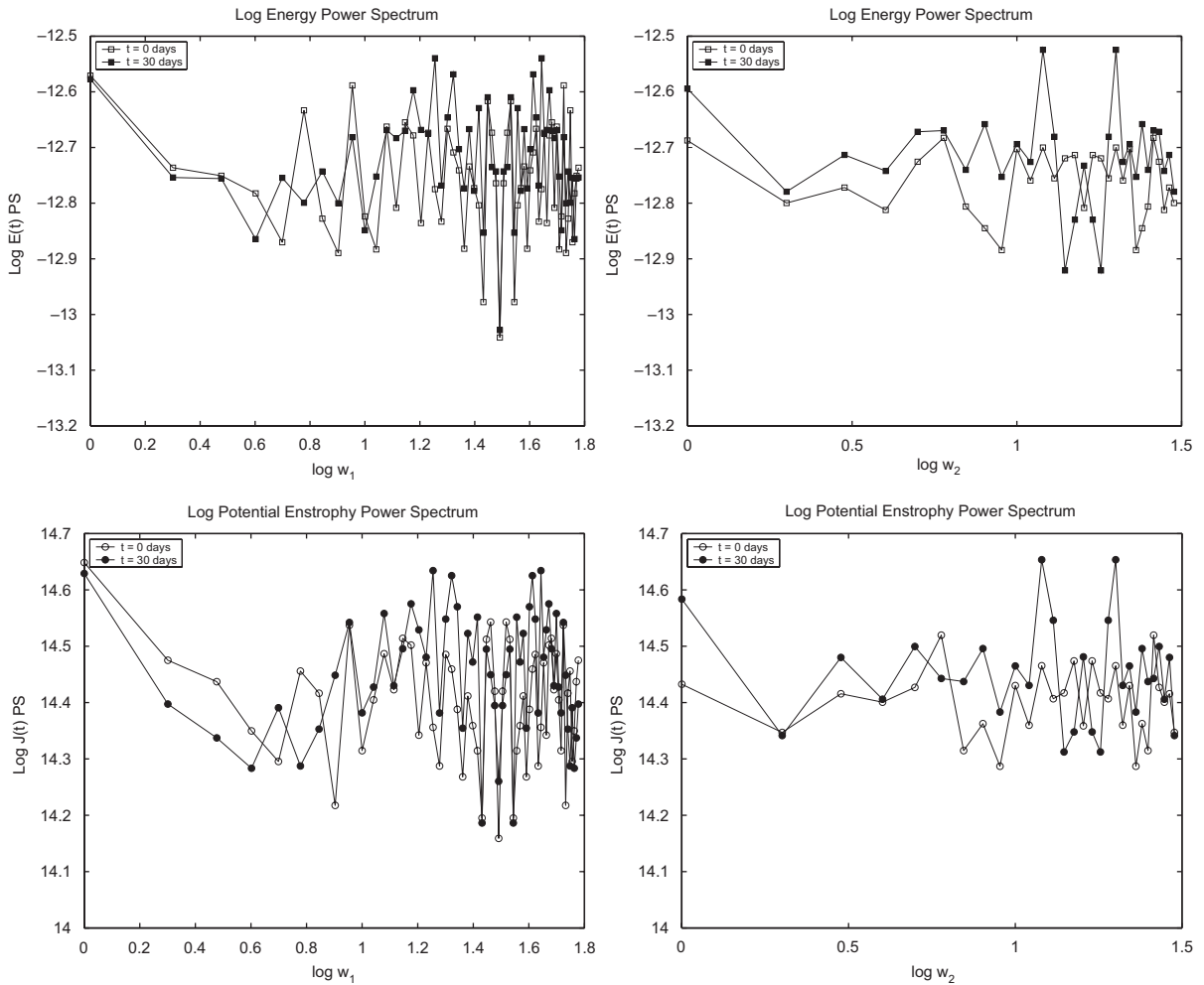
Fig. 8. Power spectra of the total energy (top) and potential enstrophy (bottom) at $t = 0$ and 30 days, fourth-order scheme. The results are averaged in ω_2 (left) and ω_1 (right).

spatial grid spacing Δr (the temporal grid spacing, τ, was being varied appropriately to keep the grid number to be of order $O(1)$). We plot these data in a logarithmic scale. For both solutions we have a power law of the form $\|\delta J(t)\|_{C[0,T]} = \Delta r^\alpha$; it is especially clear in the bottom figure ($K = \omega/10$). This, in particular, results in $\|\delta J(t)\|_{C[0,T]} \to 0$ when $\Delta r \to 0$.

In Fig. 4 we plot graphs of variations of the potential enstrophy in time. All the curves oscillate in certain intervals, without unbounded growth or decay. In Fig. 5 there are several solutions corresponding to various time moments (in days). One may see that all the fields are smooth, as it should be for RH4 waves [24].

Apart from the Rossby–Haurwitz wave, we tested the method on highly unbalanced randomly distributed initial data whose mean values satisfied the geostrophic balance with $h = 1000$ m, maximum variation of h was 80 m, and maximum velocity variation was nearly 2 m/s (cf. [12]).

On the grid $3° \times 3°$, maximum variation of the potential enstrophy was about 0.0116% for the second-order scheme and 0.0111% for the fourth-order one. In Fig. 6 we plot the graphs of $\log_{10}(J(t) - J(0))/J(0)$ for both schemes. It can be seen that the high order scheme produces a solution that moves to a $J(t)$-steady state faster than the solution provided by the low order scheme does. Yet, compared to [12], on both schemes the splitting-based approach provides more accurate results in the $J(t)$-variation (0.011% vs. 0.05%).

In Fig. 7 we plot power spectra of the total energy and potential enstrophy at $t = 0$ and 30 days corresponding to the second-order scheme (logarithmic scale). The results are averaged in frequencies ω_1, ω_2. In Fig. 8 we plot the

similar results corresponding to the fourth-order scheme. One can see that for both schemes there are no apparent energy cascades nor evident enstrophy buildups taking place at any scale—the curves at $t = 30$ days are of a chaotic behavior and resemble those at $t = 0$ days, while the latter, being consistent with the randomly distributed initial data, demonstrate the white noise.

5. Conclusion

A new method for the construction of conservative finite difference schemes for the SWM has been developed. The model was studied on a sphere. Our approach is based on the use of the method of splitting of the model equations into three simple subproblems in each (small) time interval. The splitting is accompanied with the Crank–Nicolson scheme for the discretization of each split subproblem in time. An infinite family of finite difference schemes of arbitrary order in space was constructed, which are either linear or nonlinear depending on the choice of certain parameters. Unlike all the existing schemes conserving integral characteristics when considered in semidiscrete forms, the method permits to construct fully discrete mass and total energy conservative shallow-water schemes. The method provides satisfactory numerical results on the classical Rossby–Haurwitz tests, as well as on randomly distributed shock initial conditions. Numerical implementation of the developed method is very cheap from the computational standpoint since it only requires solving linear systems with $(2N + 1)$-diagonal matrices, which can be done by employing direct band linear solvers. Yet, the joint use of the splitting method and different coordinate maps allows computing the solution on the whole sphere using the same numerical algorithm as in a doubly periodic planar domain, avoiding the question of imposing adequate boundary conditions at the poles, performing matrix bordering, or carrying out any other undesired procedures that may violate the conservation laws, reduce the solution accuracy, or increase its cost.

Acknowledgments

References

[1] A. Arakawa, V.R. Lamb, A potential enstrophy and energy conserving scheme for the shallow-water equation, Monthly Weather Rev. 109 (1981).
[2] J. Crank, P. Nicolson, A practical method for numerical evaluation of solutions of partial differential equations of the heat conduction type, Proc. Cambridge Philos. Soc. 43 (1947) 50–67.
[3] R. Jakob-Chien, et al., Spectral transform solutions to the shallow water test set, J. Comput. Phys. 119 (1995) 164–187.
[4] V.F. Kim, Numerical analysis of some conservative schemes for barotropic atmosphere, Russian Meteor. Hydrol. 6 (1984).
[5] A.N. Kolmogorov, S.V. Fomin, Elements of the Theory of Functions and Functional Analysis, Dover Publications, New York, 1999.
[6] E.N. Lorenz, The Nature and Theory of the General Circulation of the Atmosphere, World Meteorological Organization, 1967.
[7] G.I. Marchuk, Methods of Computational Mathematics, Springer, Berlin, 1982.
[8] G.I. Marchuk, Methods of Splitting, Nauka, Moscow, 1988.
[9] J. Pedlosky, Geophysical Fluid Dynamics, Springer, New York, 1982.
[10] B. Perthame, et al., A fast and stable well-balanced scheme with hydrostatic reconstruction for shallow water flows, SIAM J. Sci. Comput. 25 (2004) 2050–2065.
[11] W.H. Press, et al., Numerical Recipes in C. The Art of Scientific Computing, Cambridge University Press, Cambridge, 1992.
[12] T.D. Ringler, D.A. Randall, A potential enstrophy and energy conserving numerical scheme for solution of the shallow-water equations on a geodesic grid, Monthly Weather Rev. 130 (2002) 1397–1410.
[13] R. Sadourny, The dynamics of finite-difference models of the shallow-water equations, J. Atmospheric Sci. 32 (1975) 680–689.
[14] R. Salmon, Poisson-bracket approach to the construction of energy- and potential-enstrophy-conserving algorithms for the shallow-water equations, J. Atmospheric Sci. 61 (2004) 2016–2036.
[15] A.A. Samarskii, Yu.P. Popov, Completely conservative difference schemes, Zh. Vysshei Mat. Mat. Fiz. 9 (1969) 953–958.
[16] Yu.I. Shokin, Completely conservative difference schemes, in: G. de Vahl Devis, G. Fletcher (Eds.), Computational Fluid Dynamics, Elsevier, Amsterdam, 1988, pp. 135–155.
[17] Yu.N. Skiba, Finite-difference mass and total energy conserving schemes for shallow-water equations, Russian Meteor. Hydrol. 2 (1995) 35–43.
[18] Yu.N. Skiba, D.M. Filatov, On splitting-based mass and total energy conserving shallow-water schemes, in: International Conference on Mathematical and Numerical Aspects of Waves, SIAM, Philadelphia, PA, 2005, pp. 97–99.

[19] Yu.N. Skiba, D.M. Filatov, Conservative splitting-based schemes for numerical simulation of vortices in the atmosphere, Interciencia 31 (2006) 16–21.

[20] Yu.N. Skiba, D.M. Filatov, On splitting-based mass and total energy conserving arbitrary order shallow-water schemes, Numer. Methods Partial Differential Equations 23 (2007) 534–552.

[21] K. Takano, M.G. Wurtele, A four-order energy and potential enstrophy conserving difference scheme, Technical Report AFGL-TR-82-0205, The US Air Force Geophysics Laboratory, 1982, 85pp.

[22] C.B. Vreugdenhil, Numerical Methods for Shallow-Water Flow, Kluwer Academic Publishers, Dordrecht, 1994.

[23] D.L. Williamson, Difference approximations of flow equations on the sphere, in: Numerical Methods Used in Atmospherical Models, vol. II, GARP Publications Series, No. 17, 1979.

[24] D.L. Williamson, et al., A standard test set for numerical approximations to the shallow water equations in spherical geometry, J. Comput. Phys. 102 (1992) 211–224.